

On Two Invariants of Three Manifolds from Hopf Algebras

Liang Chang*

Chern Institute of Mathematics,
Nankai University, Tianjin 300071, China

Shawn X. Cui†

Stanford Institute for Theoretical Physics,
Stanford University, Stanford, California 94305

December 22, 2017

Abstract

We prove a 20-year-old conjecture concerning two quantum invariants of three manifolds that are constructed from finite dimensional Hopf algebras, namely, the Kuperberg invariant and the Hennings-Kauffman-Radford invariant. The two invariants can be viewed as a non-semisimple generalization of the Turaev-Viro-Barrett-Westbury (TVBW) invariant and the Witten-Reshetikhin-Turaev (WRT) invariant, respectively. By a classical result relating TVBW and WRT, it follows that the Kuperberg invariant for a semisimple Hopf algebra is equal to the Hennings-Kauffman-Radford invariant for the Drinfeld double of the Hopf algebra. However, whether the relation holds for non-semisimple Hopf algebras has remained open, partly because the introduction of framings in this case makes the Kuperberg invariant significantly more complicated to handle. We give an affirmative answer to this question. An important ingredient in the proof involves using a special Heegaard diagram in which one family of circles gives the surgery link of the three manifold represented by the Heegaard diagram.

2010 *Mathematics Subject Classification.* Primary 57M27, 16T05; Secondary 57R56

Key words and phrases Knots, 3-manifolds, quantum invariants, Hopf algebras, TQFT

*Email: changliang996@nankai.edu.cn

†Email: xingshan@stanford.edu

1 Introduction

Since the discovery of the Jones polynomial [18] and the formulation of a topological quantum field theory (TQFT)[43] [1] in the 1980s, there have been fascinating interactions between low dimensional topology and quantum physics. Many quantum invariants of 3-manifolds have been constructed, which deeply connects together different areas of research such as knot theory, tensor categories, quantum groups, Chern-Simons theory, conformal field theory, etc. Quantum invariant generally refers to the partition function of a TQFT, or less rigorously, to any invariant that is defined as a state-sum model. In dimension three, tensor categories and Hopf algebras are the main sources for quantum invariants. For instance, the Turaev-Viro-Barrett-Westbury invariant Z_{TVBW} [41] [4] and the Witten-Reshetikhin-Turaev invariant Z_{WRT} [34] are based on spherical fusion categories and modular categories, respectively. Both invariants can be extended to a TQFT and the latter is believed to be a mathematical realization of Witten-Chern-Simons theory. These invariants are particularly important in topology as they distinguish certain homotopy equivalent 3-manifolds [38].

Two fundamental invariants that are constructed from finite dimensional Hopf algebras in the early 1990s are the Kuperberg invariant Z_{Kup} [26] [27] and the Hennings-Kauffman-Radford invariant Z_{HKR} [17] [22]. On one hand, Z_{Kup} is defined for any finite dimensional Hopf algebra and is an invariant of framed oriented closed 3-manifolds. If the Hopf algebra is semisimple, then Z_{Kup} does not depend on framings and hence becomes an invariant of closed oriented 3-manifolds. On the other hand, the Z_{HKR} invariant, initially defined by Hennings and later reformulated by Kauffman and Radford, is an invariant of closed oriented 3-manifolds, but can be naturally refined to also include a 2-framing (similar to Z_{WRT}). Moreover, Z_{HKR} requires the Hopf algebra to be ribbon in addition to some non-degeneracy conditions (see Section 3.2).

The Z_{HKR} invariant has been extensively studied in the literature. In [29] [28], Lyubashenko produced an invariant from certain monoidal categories (not necessarily semisimple) which generalized both Z_{HKR} and Z_{WRT} . The relation between Z_{HKR} and Z_{WRT} for semisimple Hopf algebras and certain quantum groups were explored in [23] [10] [11] [15] [25]. TQFT properties of Z_{HKR} were given in [24] [9] [14]. Murakami combined ideas from Z_{HKR} and Z_{WRT} to define a generalized Kashaev invariant of links in 3-manifolds and proposed a version of volume conjecture for this invariant [30].

It has been a long-standing conjecture that Z_{Kup} from a Hopf algebra H is equal to Z_{HKR} from the Drinfeld double $D(H)$ of H , namely, for any closed oriented 3-manifold X ,

$$Z_{\text{Kup}}(X; H) = Z_{\text{HKR}}(X; D(H)). \quad (1)$$

The relation was speculated in [27] and stated explicitly (and more generally for Lyubashenko invariant) in [23]¹. Since then, there have been many partial results along this direction. Barrett and Westbury proved [3] that for semisimple H ,

$$Z_{\text{Kup}}(X; H) = Z_{\text{TVBW}}(X; \text{Rep}(H)). \quad (2)$$

Similarly Kerler [23] proved that for semisimple and modular H ,

$$Z_{\text{HKR}}(X; H) = Z_{\text{WRT}}(X; \text{Rep}(H)). \quad (3)$$

¹The issue of framings was not mentioned in both of these references, but we will address it below.

In this sense, Z_{Kup} and Z_{HKR} can be considered as non-semisimple generalizations of Z_{TVBW} and Z_{WRT} , respectively. If \mathcal{C} is a spherical fusion category, then the Drinfeld double $D(\mathcal{C})$ of \mathcal{C} is a modular category. Turaev and Virelizier [40] proved

$$Z_{\text{TVBW}}(X; \mathcal{C}) = Z_{\text{WRT}}(X; D(\mathcal{C})), \quad (4)$$

which generalizes the well-known result for the case of \mathcal{C} modular [42] [39] [35]

$$Z_{\text{TVBW}}(X; \mathcal{C}) = Z_{\text{WRT}}(X \# \overline{X}; \mathcal{C}). \quad (5)$$

Equations 2 3 4 together imply the conjecture in Equation 1 for semisimple Hopf algebras. A direct proof of the conjecture in this case was also given by Sequin in his thesis [37]. However, whether Equation 1 holds for non-semisimple Hopf algebras has remained to be a somewhat 20-year-old open problem. Another consequence implied from the categorical counterpart and also conjectured in [23] is that when H itself is ribbon and semisimple, we have

$$Z_{\text{Kup}}(X; H) = Z_{\text{HKR}}(X \# \overline{X}; H), \quad (6)$$

and again this has been verified directly in [7]. In the current paper, we aim to give a proof of (a suitable variation) of both Equation 1 and 6 for non-semisimple Hopf algebras. Explicitly, we prove the following two theorems.

Theorem 1.1. Let H be a finite dimensional double balanced Hopf algebra and X be a closed oriented 3-manifold, then there exist a framing b and a 2-framing ϕ of X such that,

$$Z_{\text{Kup}}(X, b; H) = Z_{\text{HKR}}(X, \phi; D(H)). \quad (7)$$

Theorem 1.2. Let H be a finite dimensional factorizable ribbon Hopf algebra and X be a closed oriented 3-manifold, then there exists a framing b of X such that

$$Z_{\text{Kup}}(X, b; H) = Z_{\text{HKR}}(X \# \overline{X}; H). \quad (8)$$

One feature of the paper is an extensive use of tensor diagrams in computing both Z_{Kup} and Z_{HKR} . In fact, both invariants can be defined by tensor diagrams alone. This implies that the results in the current paper not only hold for Hopf algebras in the category of vector spaces, but also hold for Hopf super-algebras or Hopf objects in a monoidal category which sufficiently resembles the category of finite dimensional vector spaces. For the sake of simplicity, we restrict the discussions on ordinary Hopf algebras.

These two theorems reveal a connection between Hopf algebras and 3-manifolds, which is expected to be extended as some type of duality in the category level. In one direction, Hopf algebras yield topological invariants of 3-manifolds; in the other direction, we can study Hopf algebras using topology. When the 3-manifold is fixed, Z_{Kup} and Z_{HKR} may provide algebraic invariants for Hopf algebras. Two Hopf algebras are said to be gauge equivalent if their representation categories are equivalent as tensor categories or equivalently, they are connected by the twisting of some 2-cocycle. One family of gauge invariants are the Frobenius-Schur indicators [19] [20], which have important applications to the representation theory and coincide with Z_{Kup} for lens space [8]. It is speculated that Z_{Kup} provides more general gauge invariants for any finite dimensional Hopf algebras. By a recent result on

gauge dependence of Z_{HKR} ([9]), Theorem 1.2 implies that Z_{Kup} is a gauge invariant for ribbon Hopf algebras. More detailed discussions will appear in a subsequent paper.

One issue that is not solved here is whether the 2-framing on the RHS of Equation 7 is the same as the one induced by the framing on the LHS. Since a change of 2-framing by one unit changes the Z_{HKR} by a root of unity, this issue is not relevant up to roots of unity. Another question is whether Equation 7 still holds for all framings b and the corresponding ϕ induced from b . We leave it as a future direction.

The rest of the paper is organized as follows. In Section 2 we give a review and set up the conventions on Hopf algebra. Some Lemmas on Hopf algebras will be proved for use later. Section 3 recalls the definition of the invariants Z_{Kup} and Z_{HKR} . In particular, we refine the latter to include 2-framings. Section 4 and 5 are devoted to the proof of our main results, Theorem 1.1 and Theorem 1.2, respectively.

2 Hopf Algebras

In this section we give a minimal review on Hopf algebras and prove a few lemmas. For a detailed treatment of Hopf algebras, see, for instance, [27] [32] [33], etc. Formulas in Hopf algebras are illustrated either by tensor diagrams or algebraic expressions. It is straight forward to convert one notation into the other. A novelty in this section is to represent the structure maps in the Drinfeld double by tensor diagrams from the original Hopf algebra, which turns out convenient to manipulate relations in the double and useful later in comparing different invariants of 3-manifolds. Throughout the context, Let $H = H(M, i, \Delta, \epsilon, S)$ be a finite dimensional Hopf algebra over \mathbb{C} , where the symbols inside the parenthesis denote the multiplication, unit, comultiplication, counit, and antipode, respectively.

2.1 Tensor Networks

Tensor networks have wide applications in physics and quantum information. For a review of tensor networks, see [31] [13], etc. In [26] [27], tensor networks are used as a convenient tool to represent and manipulate operations in Hopf algebras. Let V be a finite dimensional vector space and V^* be its dual. A *tensor diagram* in V is a pair $(\mathcal{G}, \mathcal{T} = \{\mathcal{T}_v\})$ where,

- \mathcal{G} is a directed graph such that at each vertex v , there is a local ordering on the set of incoming legs (i.e., edges) and a local ordering on the set of outgoing legs by $\{1, \dots, i_v\}$ and $\{1, \dots, o_v\}$, respectively;
- for each vertex v , $\mathcal{T}_v \in V^1 \otimes \dots \otimes V^{i_v} \otimes V_1 \otimes \dots \otimes V_{o_v}$, where each V^i is a copy of V^* associated with the i -th incoming leg and each V_j is a copy of V associated with the j -th outgoing leg. In this case, \mathcal{T}_v is called an (i_v, o_v) tensor.

Choose a basis $\{v_1, \dots, v_k\}$ of V and a dual basis $\{v^1, \dots, v^k\}$ of V^* , then an (m, n) tensor \mathcal{T} can be written as

$$\mathcal{T} = \sum \mathcal{T}_{i_1, \dots, i_m}^{j_1, \dots, j_n} v^{i_1} \otimes \dots \otimes v^{i_m} \otimes v_{j_1} \otimes \dots \otimes v_{j_n}. \quad (9)$$

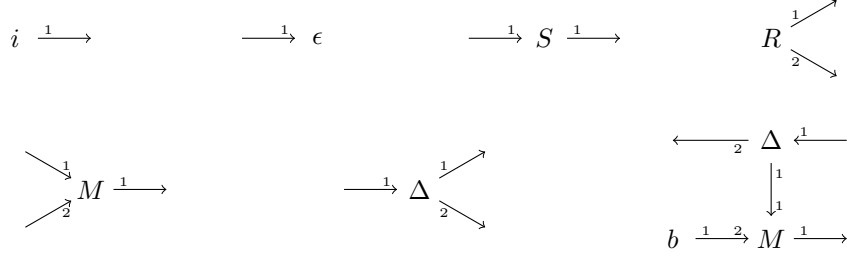


Figure 1: Examples of tensor diagrams

See Figure 1 for examples of tensor diagrams on the plane. In these diagrams, vertices are replaced by the labels of the corresponding tensors. Around a vertex, a number is placed beside each leg to represent the local ordering. An (m, n) tensor can be equivalently viewed as a linear map from $V^{\otimes m}$ to $V^{\otimes n}$. From this perspective, a $(0, 1)$ tensor is a vector, a $(1, 0)$ tensor is a co-vector, a $(1, 1)$ tensor is a linear map from V to V , etc. Let $(\mathcal{G}, \mathcal{T})$ be a tensor diagram. Assume there are $i_{\mathcal{G}} + o_{\mathcal{G}}$ dangling legs, $i_{\mathcal{G}}$ of them incoming and $o_{\mathcal{G}}$ outgoing (with a local ordering of each set), then a contraction of the tensors along all *internal* legs results in an $(i_{\mathcal{G}}, o_{\mathcal{G}})$ tensor, which we call the evaluation of $(\mathcal{G}, \mathcal{T})$. By abuse of language, we do not distinguish a tensor diagram with its evaluation.

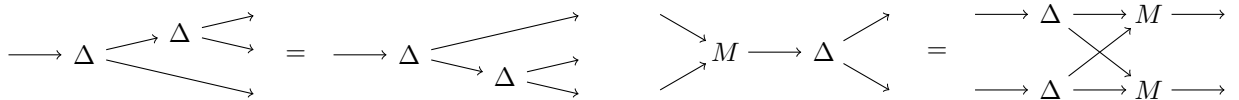
Now we make an important convention to simplify drawing tensor diagrams. At each vertex of a tensor diagram, we always group the incoming legs and the outgoing legs. Unless noted otherwise, incoming legs are enumerated *counter clockwise* and outgoing legs *clockwise*. This uniquely determines a local ordering if both types of legs are present:



If there is only one type of legs and the tensor is neither a $(1, 0)$ tensor nor a $(0, 1)$ tensor, we mark the leg labeled by 1 explicitly to avoid ambiguities:



If $V = H$ is a Hopf algebra, the tensor diagrams of the structure maps are represented by those with the corresponding labels in Figure 1. Relations of between these maps can also be illustrated in tensor diagrams. For instance, the equations $(\Delta \otimes id) \circ \Delta = (id \otimes \Delta) \circ \Delta$ and $\Delta \circ M = (M \otimes M) \circ (id \otimes P \otimes id) \circ (\Delta \otimes \Delta)$ are represented by:



where $P : H \otimes H \rightarrow H \otimes H$ is the swap map. For $n \geq 1$, denote the tensor diagrams for the maps $(\Delta \otimes id^{\otimes(n-2)}) \circ \dots \circ (\Delta \otimes id) \circ \Delta$ and $M \circ (M \otimes id) \circ \dots \circ (M \otimes id^{\otimes(n-2)})$ by:

$$\longrightarrow \Delta \begin{array}{l} \nearrow 1 \\ \nearrow 2 \\ \searrow \\ \searrow n \end{array} \quad \dots \quad \begin{array}{l} \nearrow 1 \\ \nearrow 2 \\ \searrow \\ \searrow n \end{array} M \longrightarrow \quad (10)$$

An (m, n) tensor \mathcal{T} in V can also be viewed as an (n, m) tensor \mathcal{T}^* in V^* by

$$\mathcal{T}^*_{j_1, \dots, j_n}^{i_1, \dots, i_m} := \mathcal{T}_{i_1, \dots, i_m}^{j_1, \dots, j_n}. \quad (11)$$

If \mathcal{T} is interpreted as a map from $V^{\otimes m}$ to $V^{\otimes n}$, then \mathcal{T}^* is the dual map of \mathcal{T} . For instance, if $V = H$ is a Hopf algebra, then Δ^* is a $(2, 1)$ tensor representing the multiplication in V^* and for $f, f' \in V^*$, $\Delta^*(f \otimes f')$ is given by:

$$\begin{array}{c} f \\ \diagdown \quad \diagup \\ \quad \quad \Delta \longleftarrow \\ \diagup \quad \diagdown \\ f' \end{array} \quad (12)$$

Note that there is a swap of the two outgoing legs in the above diagram because of our convention for the implicit ordering of the incoming/outgoing legs. The dual notion of tensors will be used in Section 2.4 when dealing with the quantum double of Hopf algebras.

2.2 Integrals in Hopf Algebras

A left (resp. right) integral of H is an element $e_L \in H$ (resp. $e_R \in H$) such that $xe_L = \epsilon(x)e_L$ (resp. $e_Rx = \epsilon(x)e_R$) for any $x \in H$. Left and right integrals of H^* are denoted by μ_L and μ_R , respectively. The defining equations of e_L, e_R, μ_L , and μ_R ² in terms of tensor diagrams are given by:

$$\begin{array}{ccc} \begin{array}{c} \diagdown \\ \quad M \longrightarrow \\ \diagup \\ e_L \end{array} \longrightarrow & = & \longrightarrow \epsilon e_L \longrightarrow \\ \begin{array}{c} \longrightarrow \Delta \\ \diagup \quad \diagdown \\ \mu_L \end{array} & = & \longrightarrow \mu_L i \longrightarrow \end{array} \quad \begin{array}{ccc} \begin{array}{c} e_R \diagdown \\ \quad M \longrightarrow \\ \diagup \\ \end{array} \longrightarrow & = & \longrightarrow \epsilon e_R \longrightarrow \\ \begin{array}{c} \longrightarrow \Delta \\ \diagup \quad \diagdown \\ \mu_R \end{array} & = & \longrightarrow \mu_R i \longrightarrow \end{array} \quad (13)$$

The space of left integrals and the space of right integrals are both one dimensional. Choose right integrals $e_R \in H, \mu_R \in H^*$ such that $\mu_R(e_R) = 1$. Define the distinguished group-like elements $a \in H, \alpha \in H^*$ by,

$$a \longrightarrow := e_R \longrightarrow \begin{array}{c} \diagup \\ \quad \Delta \\ \diagdown \\ \mu_R \end{array} \quad \longrightarrow \alpha := \begin{array}{c} \diagdown \\ \quad M \longrightarrow \mu_R \\ \diagup \\ e_R \end{array} \quad (14)$$

and for $n \in \mathbb{Z}$ define $\mu_{n-\frac{1}{2}} \in H^*, e_{n-\frac{1}{2}} \in H$ by

$$\longrightarrow \mu_{n-\frac{1}{2}} := \begin{array}{c} \diagdown \\ \quad M \longrightarrow \mu_R \\ \diagup \\ a^n \end{array} \quad e_{n-\frac{1}{2}} \longrightarrow := e_R \longrightarrow \begin{array}{c} \diagup \\ \quad \Delta \\ \diagdown \\ \alpha^n \end{array} \quad (15)$$

Then $\mu_R = \mu_{-\frac{1}{2}}, e_R = e_{-\frac{1}{2}}$ are right integrals and $\mu_L := \mu_{\frac{1}{2}}, e_L := e_{\frac{1}{2}} \in H$ are left integrals. Set $q := \alpha(a)$. It follows that q is a root of unity and we have $\mu_R(e_R) =$

²In [27] they are called left cointegral, right cointegral, left integral and right integral, respectively, of H .

$\mu_R(e_L) = \mu_L(e_R) = 1$ and $\mu_L(e_L) = q^{-1}$. Moreover, $\mu_L \circ S = \mu_R$, $\mu_R \circ S = q\mu_L$, $S(e_L) = e_R$, $S(e_R) = qe_L$. Thus S^2 has eigenvalue q on all integrals of H and H^* . The relations between integrals and the distinguished group-like elements are given as follows:

$$\begin{array}{ccc}
\begin{array}{c} \nearrow \\ M \longrightarrow \\ \nwarrow \\ e_R \end{array} & = & \longrightarrow \alpha e_R \longrightarrow \\
\begin{array}{c} \nearrow \\ M \longrightarrow \\ \nwarrow \\ e_L \end{array} & = & \longrightarrow \alpha^{-1} e_L \longrightarrow \\
\longrightarrow \Delta \begin{array}{c} \nearrow \\ \nwarrow \\ \mu_R \end{array} & = & \longrightarrow \mu_R a \longrightarrow \\
\longrightarrow \Delta \begin{array}{c} \nearrow \\ \nwarrow \\ \mu_L \end{array} & = & \longrightarrow \mu_L \alpha^{-1} \longrightarrow
\end{array} \tag{16}$$

Note that here a and α correspond to g and α^{-1} , respectively, in [32] [33]. The well-known Radford formula for S^4 can be expressed as

$$\longrightarrow S^4 \longrightarrow = \begin{array}{c} a \nearrow \\ \longrightarrow M \longrightarrow \Delta \begin{array}{c} \nearrow \\ \longrightarrow \\ \nwarrow \\ \alpha^{-1} \end{array} \\ \alpha^{-1} \nwarrow \end{array} \begin{array}{c} \alpha \\ \longrightarrow \\ \alpha^{-1} \end{array} \tag{17}$$

Also define

$$\longrightarrow T \longrightarrow := \longrightarrow S^{-2} \longrightarrow \Delta \begin{array}{c} \alpha \\ \longrightarrow \\ \alpha^{-1} \end{array} \tag{18}$$

Then T is an automorphism of H as a Hopf algebra, i.e., T commutes with all structure maps of H .

Lemma 2.1. For any $n \in \mathbb{Z}$,

- S^2 has eigenvalue q on $e_{n-\frac{1}{2}}$ and $\mu_{n-\frac{1}{2}}$, namely, $S^2(e_{n-\frac{1}{2}}) = qe_{n-\frac{1}{2}}$, $\mu_{n-\frac{1}{2}} \circ S^2 = q\mu_{n-\frac{1}{2}}$.
- T fixes a , α , $e_{n-\frac{1}{2}}$, $\mu_{n-\frac{1}{2}}$, namely, $T(a) = a$, $\alpha \circ T = \alpha$, $T(e_{n-\frac{1}{2}}) = e_{n-\frac{1}{2}}$, $\mu_{n-\frac{1}{2}} \circ T = \mu_{n-\frac{1}{2}}$.

Proof. The first part follows directly from the calculation:

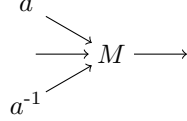
$$e_R \longrightarrow \Delta \begin{array}{c} \nearrow S^2 \\ \nwarrow \alpha^n \end{array} = e_R \longrightarrow S^2 \longrightarrow \Delta \begin{array}{c} \nearrow \\ \nwarrow \alpha^n \end{array} = q e_R \longrightarrow \Delta \begin{array}{c} \nearrow \\ \nwarrow \alpha^n \end{array}$$

For the second part, $\mu_R \circ (S^2T)$ is computed as follows:

$$\longrightarrow \Delta \begin{array}{c} \alpha \\ \longrightarrow \mu_R \\ \nwarrow \alpha^{-1} \end{array} = \longrightarrow \Delta \begin{array}{c} \alpha \\ \longrightarrow \alpha^{-1}(1) \\ \nwarrow \mu_R \end{array} = \longrightarrow \mu_R(q)$$

where the first equality is by definition of μ_R and the second equality is by Equation 16. Hence $\mu_R \circ (S^2T) = q\mu_R$. By the first part, we have $\mu_R \circ T = \mu_R$.

By using the Radford formula in Equation 17, S^2T^{-1} can be expressed as



A similar calculation as above shows that $S^2T^{-1}(e_R) = qe_R$, and thus $T(e_R) = e_R$. That T also fixes $e_{n-\frac{1}{2}}$ and $\mu_{n-\frac{1}{2}}$ follows immediately. \square

The Hopf algebra H is called *balanced* if $T = id$, and *unimodular* if left integrals of H are also right integrals. The latter is equivalent to the condition that $\alpha = \epsilon$. If H is unimodular, then $q = 1$, $e_L = e_R \in Z(H)$, and for any $x, y \in H$, we have

$$\mu_R \circ S^2(x) = \mu_R(x), \quad \mu_R(xy) = \mu_R(S^2(y)x) = \mu_R(yS^{-2}(x)). \quad (19)$$

2.3 Ribbon Hopf Algebras

A *quasitriangular* Hopf algebra is a pair (H, R) , where H is a finite dimensional Hopf algebra, $R \in H \otimes H$, called the R -matrix, is an invertible element, and for any $x \in H$,

$$R\Delta(x) = \Delta^{\text{op}}(x)R, \quad (\Delta \otimes id)(R) = R_{13}R_{23}, \quad (id \otimes \Delta)(R) = R_{13}R_{12}. \quad (20)$$

If (H, R) is quasitriangular, then

$$R^{-1} = (S \otimes id)(R) = (id \otimes S^{-1})(R), \quad R = (S \otimes S)(R), \quad (\epsilon \otimes id)(R) = (id \otimes \epsilon)(R) = 1. \quad (21)$$

Let $u := M \circ (S \otimes id)(R_{21}) \in H$ be the *Drinfeld element*. Then u is invertible and $S^2(x) = uXu^{-1}$ for any $x \in H$. Moreover, $S(u)u = uS(u) \in Z(H)$, and if H is unimodular, then $uS(u)^{-1} = a$ is the distinguished group-like element. Set $Q = R_{21}R$ and define the Drinfeld map f_Q by

$$f_Q : H^* \longrightarrow H, \quad p \longmapsto (p \otimes id)Q.$$

Then $f_Q(\alpha^{-1}) = 1 = f_Q(\epsilon)$.

The pair (H, R) is called *factorizable* if (H, R) is quasitriangular and f_Q is a linear isomorphism. Thus factorizable Hopf algebras are unimodular, with the distinguished group element given by $uS(u)^{-1}$. Let (H, R) be factorizable and μ_R be a right integral, then $f_Q(\mu_R)$ is a (two-sided) integral of H and one can choose μ_R such that $\mu_R \circ f_Q(\mu_R) = 1$.

A ribbon Hopf algebra is a triple (H, R, v) where (H, R) is a quasitriangular Hopf algebra and $v \in Z(H)$, called the ribbon element, satisfies the following equation:

$$v^2 = uS(u), \quad S(v) = v, \quad \epsilon(v) = 1, \quad \Delta(v) = (v \otimes v)Q^{-1}. \quad (22)$$

Since u is invertible, so is v . Let $G := uv^{-1}$. Then G is a group-like element and $G^2 = u^2v^{-2} = uS(u)^{-1}$.

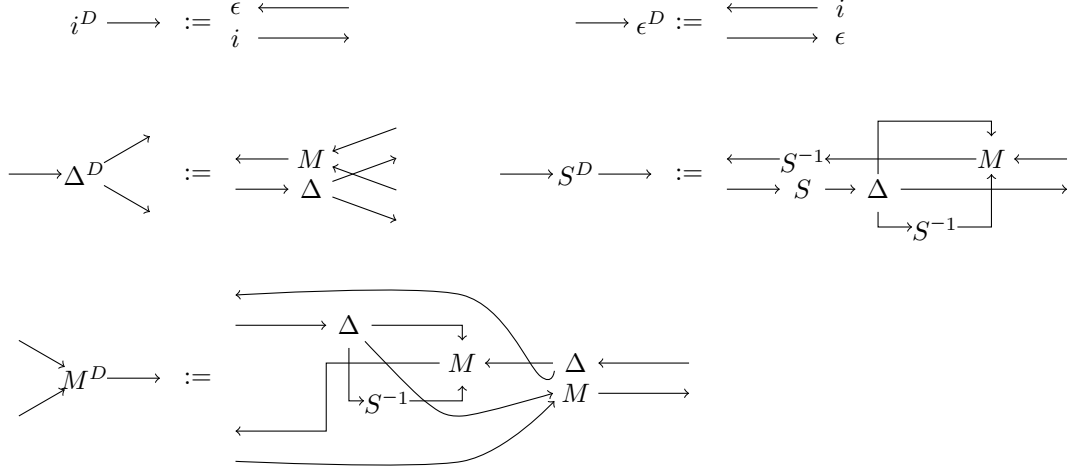


Figure 2: Definition of Hopf algebra structures in $D(H)$



Figure 3: The R -matrix in $D(H)$, where $\overline{R^D}$ means $(R^D)^{-1}$.

2.4 The Quantum Double of Hopf Algebras

Introduced in [16], the quantum double (or Drinfeld double) $D(H) = H^{*\text{cop}} \otimes H$ of a Hopf algebra H is a factorizable quasitriangular (and thus unimodular) Hopf algebra. Instead of writing down algebraically the Hopf algebra structures in $D(H)$, we describe them with tensor diagrams consisting of tensors in H , which will be used later in Section 4 to describe the Z_{HKR} invariant from a quantum double. Labels for operations in the double will be endowed with a superscript ‘ D ’. For instance, Δ^D means the comultiplication in $D(H)$. The vector $f \otimes v \in D(H)$ and covector $v \otimes f \in D(H)^*$ are represented respectively by

$$\begin{array}{ccc} f \longleftarrow & & \longleftarrow v \\ v \longrightarrow & & \longrightarrow f \end{array} \quad (23)$$

That is, we use a pair of oppositely directed arrows to represent a copy of $D(H)$ with the arrow on the top corresponding to $H^{*\text{cop}}$ and the one on the bottom to H . The definition of the Hopf algebra structures in $D(H)$ using tensor diagrams are given in Figure 2. Keep in mind that for a tensor with both incoming and outgoing legs, the incoming legs are listed in *counter-clockwise* order while the outgoing legs *clockwise*. The R -matrix is given in Figure 3.

One advantage of using tensor diagrams is that it provides a direct visualization on how structures in the double are constructed from those in the original Hopf algebra. It is also convenient for deriving equations. Of course, one can always obtain the algebraic expressions from the diagrams. For instance, for $f \otimes v, f' \otimes v' \in D(H)$, from Figure 2 we see the the

In [9], this condition is called *double balanced*, but this is not to be confused with the *balanced* condition defined in Section 2.2. It is direct to see that $\tau := \beta(b)$ is a fourth root of q . The corresponding ribbon element of $D(H)$ is given by:

$$v^D := \begin{array}{c} \beta \longleftarrow \Delta \longleftarrow \\ b \longrightarrow M \longleftarrow S \longrightarrow \end{array} \quad (v^D)^{-1} := \begin{array}{c} \beta^{-1} \longleftarrow \Delta \longleftarrow \\ b^{-1} \longrightarrow M \xleftarrow{\bar{S}} S \longrightarrow \end{array} \quad (29)$$

where \bar{S} in the above diagram means S^{-1} .

By direct calculations, $G^D = \beta^{-1} \otimes b$, $\mu_R^D(v^D) = \tau^{-5}$, $\mu_R^D((v^D)^{-1}) = \tau$.

3 Invariants from Hopf Algebras

In this section we review and make some clarifications on the definitions of the Kuperberg invariant and the Hennings-Kauffman-Radford invariant.

3.1 Kuperberg Invariant Z_{Kup}

The Kuperberg invariant is defined for closed framed oriented 3-manifolds from a finite dimensional Hopf algebra [27]. If the Hopf algebra is semi-simple, then the invariant becomes independent of the framings, and is reduced to the invariant of closed oriented 3-manifolds in [26].

We first recall the definitions of combings, framings, and their representations on Heegaard diagrams. Let X be a closed oriented 3-manifold endowed with a Riemannian metric. A *combing* of X is a unit-norm vector field considered up to homotopy, and a *framing* of X consists of three orthonormal vector fields consistent with the orientation, again considered up to homotopy. Since the tangent bundle of X is trivial, the set of combings (resp. framings) correspond to homotopy classes of maps from X to \mathbb{S}^2 (resp. $\text{SO}(3)$), although the correspondence is in general not canonical. Let $R = (\Sigma_g, \alpha, \beta)$ be a Heegaard diagram of X where Σ_g is a closed oriented surface of genus g , and α and β are the collection of lower circles and upper circles, respectively. We only consider minimal Heegaard diagrams. That is, α and β each contains exactly g circles. In the following, R and Σ_g will be used interchangeably when no confusion arises. Different diagrams of X are related by circle slide, stabilization, and isotopy. Let \vec{n} be the unit normal vector field of Σ_g in X pointing from the lower handlebody to the upper handlebody. By convention, the orientation on Σ_g and \vec{n} form the orientation on X . Any vector field on X can be orthogonally projected along \vec{n} to a tangent vector field on Σ_g , which could have singularities. The converse problem of extending a vector field on Σ_g with certain properties to one on X is studied in [27].

According to [27], any combing of X can be represented by a combing of Σ_g , which, by definition, is a vector field on Σ_g with $2g$ singularities of index -1 , one on each circle, and one more singularity of index 2 disjoint from all circles. Moreover, each singularity of index -1 is distinct from all crossings of the circles, and the two out-pointing vectors should be tangent to the circle. See Figure 5 for the local geometry of singularities and the circle near the singularity on it. Any combing b of Σ_g can be extended to a combing \tilde{b} of X whose projection to Σ_g is the same as b , and moreover, one can choose \tilde{b} in such a way that it coincides with b on Σ_g away from a small neighborhood of singularities, and at the singularity on a lower (resp. upper) circle \tilde{b} is opposite (resp. parallel) to \vec{n} .

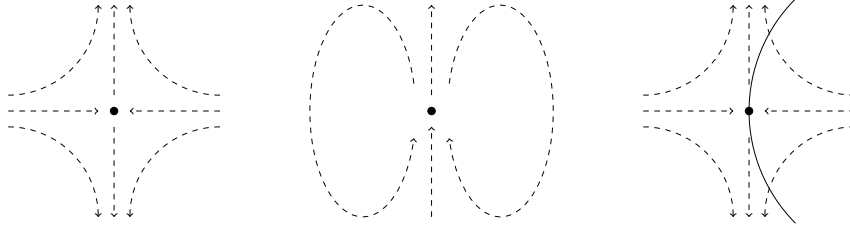


Figure 5: (Left) Singularity of index -1 ; (Middle) Singularity of index 2 ; (Right) Local picture of a circle (solid curve) near the singularity.

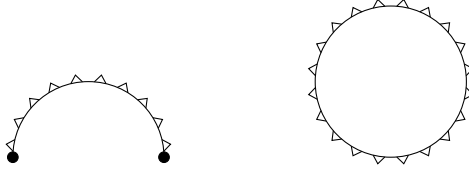


Figure 6: An illustration of twist fronts.

A framing of X is determined by two orthonormal combings $(\tilde{b}_1, \tilde{b}_2)$ since the third one can be inferred from the first two and the orientation. By the previous argument, we can represent the framing as two orthogonal combings (b_1, b_2) on Σ_g . For reasons that will become clear below, we represent b_2 in a different but equivalent form to a combing. Let Σ_g^* be the punctured surface of Σ_g with all singularities of b_1 removed. Then $(b_1, \vec{n}, b_1 \times \vec{n})$ forms an orthogonal frame on Σ_g where $b_1 \times \vec{n}$ is the vector orthogonal to both b_1 and \vec{n} such that the triple $(b_1, \vec{n}, b_1 \times \vec{n})$ matches the orientation of X . Since b_2 is orthogonal to b_1 , b_2 lies in the plane spanned by \vec{n} and $b_1 \times \vec{n}$. Then we can define a map $f : \Sigma_g^* \rightarrow \mathbb{S}^1$ by sending x to $f(x) = (f_1(x), f_2(x))$ such that,

$$b_2(x) = f_1(x)\vec{n} + f_2(x)b_1 \times \vec{n}.$$

By perturbing b_2 in general position, one can assume $(1, 0)$ is a regular value of f and hence $f^{-1}(1, 0)$ is a 1-manifold. Namely, the set of points at which b_2 is parallel to \vec{n} is a 1-manifold, where each connected component is either a simple closed curve or an open curve approaching to some singularities in both directions. We also attach small triangles (See figure 6) on one side of the curves to indicate the direction in which b_2 is rotating about b_1 by the right-hand rule. More specifically, f takes values in the first quadrant at points which are close to the curve and are located on the side of the curve with triangles. The curves with small triangles attached are called *twist fronts*. Twist fronts determine b_2 on Σ_g . Given a collection of twist fronts indicating b_2 , the following condition needs to be satisfied in order to extend b_2 to a combing on X orthogonal to \tilde{b}_1 .

Arbitrarily orient all circles and consider the frame $(\vec{n}, b_1, \vec{n} \times b_1)$ on Σ_g^* . For each lower or upper circle c , the tangent vector field c' lies in the plane spanned by b_1 and $\vec{n} \times b_1$. Define θ_c to be the total counter-clockwise rotation, in unit of $1 = 360^\circ$, of c' relative to b_1 in the direction of c ³. Note that near the singularity c' is parallel to b_1 in the forward

³Strictly speaking, the rotation of c' around b_1 at the singularity does not make sense since b_1 vanishes. Then θ_c is actually defined as the limit $\lim_{x \rightarrow *, y \rightarrow *} \theta_{c[x, y]}$, where ‘*’ is the singularity on c , x (resp. y) is a

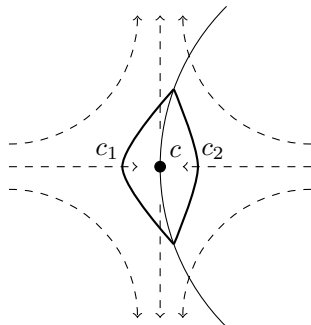


Figure 7: Perturbation of a circle c off its singularity.

direction and anti-parallel to b_1 in the backward direction, thus θ_c is always a proper half integer. A crossing of a circle with a twist front is called positive if the circle travels from the non-triangle side to the triangle side, and is negative otherwise. Define ϕ_c to be the number of signed crossings of c with twist fronts, with the crossings at the singularity counted half as much. Then the condition b_1 and b_2 need to satisfy is:

$$\theta_c = \begin{cases} \phi_c & , c \text{ is a lower circle} \\ -\phi_c & , c \text{ is an upper circle} \end{cases} \quad (30)$$

Remark 3.1. A more intrinsic way to define ϕ_c is to use total rotations similar to the definition of θ_c . There are two ways to perturb the circle c off its singularity. See Figure 7. Let c_1 and c_2 denote the circles resulting from the two perturbations, hence they are contained in Σ_g^* . Consider the orthogonal frame $(b_1, \vec{n}, b_1 \times \vec{n})$ on Σ_g^* . Note that b_2 lies in the plane spanned by \vec{n} and $b_1 \times \vec{n}$. Define ϕ_{c_i} to be the total counter-clockwise rotation of b_2 relative to \vec{n} along the curve c_i . Then one can check that ϕ_{c_i} equals the number of signed crossings of c_i with twist fronts, and the previously defined ϕ_c is $\frac{\phi_{c_1} + \phi_{c_2}}{2}$.

Let p be a point on a c . Define $\theta_c(p)$ to be the counter-clockwise rotation of c' relative to b_1 going along the circle from the singularity to p , and define $\phi_c(p)$ to be the number of signed crossings of c with twist fronts from a point near the singularity in the forward direction to p . Arrange the diagram so that lower circles intersect upper circles orthogonally. If p is the point of crossing of the lower circle l with the upper circle u , let

$$\theta(p) := 2(\theta_l(p) - \theta_u(p)) + \frac{1}{2}, \quad \phi(p) := \phi_l(p) - \phi_u(p). \quad (31)$$

It can be shown that $\theta(p)$ is always an integer. Actually, $\theta(p)$ is even if and only if l and u form a positive basis of the tangent space at p . We note that in the original definition of $\theta(p)$ in [27], the last term is $-\frac{1}{2}$ instead of $\frac{1}{2}$, but we will stick to the current convention as only with this convention, the invariant to be defined will reduce to the one introduced in [26] when the Hopf algebra is semi-simple.

We are ready to define the Kuperberg invariant. Let H be a finite dimensional Hopf algebra. We will use notations from Section 2. Choose a right integral μ_R and a right point of c near the singularity in the forward (resp. backward) direction, and $c[x, y]$ is the subarc of c from x to y . Similar situation applies to the definition of $\theta_c(p)$ for a point p on c to be introduced below

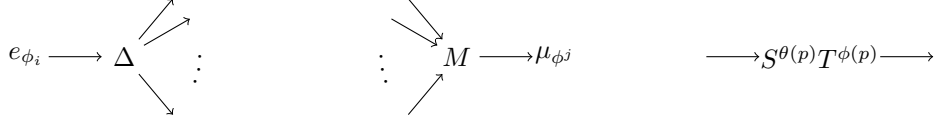


Figure 8: (Left) the Δ tensor assigned to α_i ; (Middle) the M tensor assigned to β_j ; (Right) the ST tensor assigned to a crossing p .

co-integral e_R so that $\mu_R(e_R) = 1$, and recall the definitions of μ_n, e_n for n a half integer. Let X be a closed orientated 3-manifold with a framing $b = (b_1, b_2)$ given on a Heegaard diagram $R = (\Sigma_g, \alpha, \beta)$, where $\alpha = \{\alpha_1, \dots, \alpha_g\}$ and $\beta = \{\beta_1, \dots, \beta_g\}$ are lower and upper circles, respectively. Orient all circle arbitrarily, and call the singularity on each circle the basepoint. The definition of the Kuperberg invariant is best illustrated using tensors and tensor contractions. We also given an alternative way to interpreted it afterwards.

For each lower circle α_i , let $\phi_i = \phi_{\alpha_i} (= \theta_{\alpha_i})$ and assign the tensor in Figure 8(Left) to α_i , one leg for each crossing on α_i counted from the basepoint along its orientation. Similarly for each upper circle β_j , let $\phi^j = \phi_{\beta_j} (= -\theta_{\beta_j})$ and assign the tensor in Figure 8(Middle) to β_j . For each crossing p , insert the tensor shown in Figure 8(Right) to connect the two legs, one from the tensor of the lower circle and one from the tensor of the upper circle. Then one obtains a tensor network consisting of the three families of tensors from Figure 8 without free legs. The Kuperberg invariant $Z_{\text{Kup}}(X, b; H)$ is then defined to be the contraction of this tensor network.

A more ‘algebraic’ but also more lengthy way to define the invariant is as follows. Enumerate the crossings by p_1, p_2, \dots, p_m . Let

$$H_\alpha = \bigotimes_{i=1}^g H(\alpha_i), \quad H_\beta = \bigotimes_{i=1}^g H(\beta_i), \quad H_c = \bigotimes_{i=1}^m H(p_i), \quad (32)$$

Where each $H(\cdot)$ is a copy of H . For each lower circle α_i , let p_{i_1}, \dots, p_{i_k} be the crossings on α_i listed from the base point along its orientation, and let $H_c(\alpha_i) = \bigotimes_{n=1}^k H(p_{i_n})$. Define $H_c(\beta_j)$ in a similar way. It follows that

$$H_c = \bigotimes_{i=1}^g H_c(\alpha_i) = \bigotimes_{j=1}^g H_c(\beta_j), \quad (33)$$

up to a permutation of tensor components. Define

$$\Delta_i : H(\alpha_i) \longrightarrow H_c(\alpha_i), \quad x \longmapsto x^{(1)} \otimes \dots \otimes x^{(k)} \quad (34)$$

$$M_j : H_c(\beta_j) \longrightarrow H(\beta_j), \quad x_1 \otimes \dots \otimes x_k \longmapsto x_1 \cdots x_k \quad (35)$$

$$C_n : H(p_n) \longrightarrow H(p_n), \quad x \longmapsto S^{\theta(p_n)} T^{\phi(p_n)}(x) \quad (36)$$

Then $Z_{\text{Kup}}(X, b; H)$ is defined by

$$Z_{\text{Kup}}(X, b; H) = \left(\bigotimes_{j=1}^g \mu_{\phi^j} \circ M_j \right) \left(\bigotimes_{n=1}^m C_n \right) \left(\bigotimes_{i=1}^g \Delta_i(e_{\phi_i}) \right). \quad (37)$$

3.2 Hennings-Kauffman-Radford Invariant Z_{HKR}

For a finite dimensional unimodular ribbon Hopf algebra (H, R, v) with certain non-degeneracy condition, a topological invariant of closed oriented 3-manifolds was constructed by Hennings [17] and later reformulated by Kauffman and Radford [22].

Given a non-zero right integral $\mu_R \in H^*$, one can associate a regular isotopy invariant $\langle L \rangle_{H, \mu_R}$ to a framed unoriented link L as follows. Choose a link diagram of L (still denoted by L) with respect to a height function such that the crossings are not critical points. On each component L_i of L , pick a base point which is neither a crossing nor an extremum, and arbitrarily orient L_i . Define δ_i to be 0 if the orientation of L_i near the base point is downwards and 1 otherwise. For a point p on L_i which is not an extremum, let w_p be the algebraic sum of extrema between the base point and p , where an extremum is counted as +1 (resp. -1) if the orientation near it is counterclockwise (resp. clockwise). Equivalently, w_p is 2 times the total counterclockwise rotation, in unit of $1 = 360^\circ$, of the tangent of L_i from the base point to p . Define w_i to be $\frac{w_p}{2}$ for p very close to the base point in the backward direction of L_i . Clearly, w_i is equal to the winding number of L_i . Decorate each crossing with the tensor factors of the R -matrix $R = \sum_i s_i \otimes t_i$ as below.⁴



Then we replace each decorating element x on L_i by $S^{-w_{p(x)} + \delta_i}(x)$, where $p(x)$ denotes the point on L_i where x is located. See below for the contribution of each extremum to the powers of S .



Then $\langle L \rangle_{H, \mu_R}$ is the evaluation of the right integral μ_R on the products along each L_i :

$$\langle L \rangle_{H, \mu_R} := \sum_{(R)} \mu_R(q_1 G^{1-w_1}) \cdots \mu_R(q_{c(L)} G^{1-w_{c(L)}}), \quad (38)$$

where $c(L)$ is the number of components of L , $q_i \in H$ is the product of the decorating elements (after applying S -powers) on L_i multiplied in the order following its orientation starting from the base point.

It can be checked that $\langle L \rangle_{H, \mu_R}$ is independent of the choice of base points, orientation, and the height function. It is also preserved under framed Reidemeister moves. Thus $\langle \cdot \rangle_{H, \mu_R}$ defines an invariant of framed links.

⁴After a crossing is decorated by the R -matrix elements, the over/under crossing information becomes irrelevant and we sometimes simply replace it by a solid crossing. But this is only a notation preference. In the tensor network formulation below, we will still keep the crossing as it is.

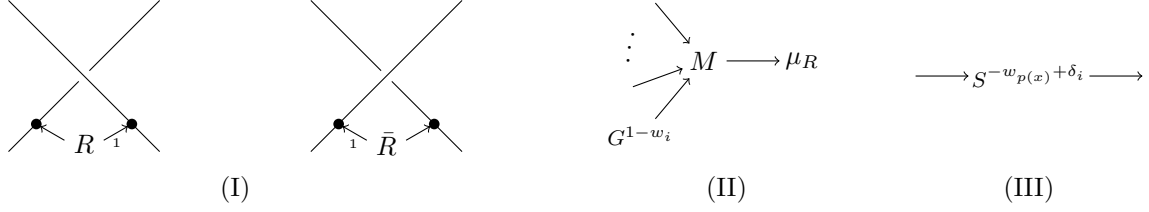


Figure 9: Tensors associated with a link diagram, where \bar{R} means R^{-1} .

- Remark 3.2.**
1. The notation here is different from but essentially the same as the Kauffman and Radford's version where the decorating elements are pushed to a vertical portion and multiplied together from bottom to top.
 2. Since $(S \otimes S)(R) = R$ and $\mu_R \circ S^2 = \mu$, one can also replace δ_i with $1 - \delta_i$ in the definition of $\langle L \rangle_{H, \mu_R}$. However, this replacement has to be performed on all components of L simultaneously.
 3. If we restrict to the class of even framed links, namely, framed links where each component has an even framing, it can be shown that in any diagram of such links the winding number of each component is odd. Noting that $G^2 = uS(u^{-1})$, $\langle L \rangle_{H, \mu_R}$ can be rewritten as

$$\langle L \rangle_{H, \mu_R} := \sum_{(R)} \mu_R \left(q_1 (uS(u^{-1}))^{\frac{1-w_1}{2}} \right) \cdots \mu_R \left(q_{c(L)} (uS(u^{-1}))^{\frac{1-w_{c(L)}}{2}} \right).$$

Hence, $\langle L \rangle_{H, \mu_R}$ does not depend on the ribbon structure of H and can be defined for any unimodular quasitriangular Hopf algebras. See [36].

Equivalently, it is convenient to describe $\langle L \rangle_{H, \mu_R}$ in the language of tensor networks. Again choose a base point and an orientation for each component. To each crossing assign an R -tensor according to the rule in Figure 9 (I). The first leg of the R - or R^{-1} -matrix always corresponds to the over-crossing strand. The legs terminate at links with a dot (see Figure 9 (I)). To each component L_i assign an \widetilde{M} -tensor as shown in Figure 9 (II), one leg for each dot on L_i listed from the base point along its orientation. At each dot of L_i , insert an S -tensor as shown in Figure 9 (III) connecting the leg from the R -tensor to the leg from the \widetilde{M} -tensor. Then $\langle L \rangle_{H, \mu_R}$ is equal to the contraction of these tensors.

It is a direct calculation that the invariant of the unknot with framing ± 1 is $\mu_R(v^{\pm 1})$. From now on assume $\mu_R(v)\mu_R(v^{-1}) \neq 0$, which is the non-degeneracy condition we impose on H and which is always true when H is factorizable [12]. Let $\omega(v)$ be a square root of $\mu_R(v)/\mu_R(v^{-1})$, then $\mu_R(v)/\omega(v)$ is a square root of $\mu_R(v)\mu_R(v^{-1})$. The Z_{HKR} invariant for a closed oriented 3-manifold X is defined to be:

$$Z_{\text{HKR}}(X; H, \omega(v)) = (\mu_R(v)/\omega(v))^{-c(L)} \omega(v)^{-\text{sign}(L)} \langle L \rangle_{H, \mu_R}, \quad (39)$$

where L is a surgery link of X and $\text{sign}(L)$ denotes the signature of the framing matrix of L .

Remark 3.3. By its very definition, $\omega(v)$ does not depend on μ_R . For any non-zero scalar $s \in \mathbb{C}$, clearly we have $\langle L \rangle_{H, s\mu_R} = s^{c(L)} \langle L \rangle_{H, \mu_R}$. It follows that $Z_{\text{HKR}}(X; H, \omega(v))$ does not depend on μ_R either. If one chooses the other square root $-\omega(v)$, then

$$Z_{\text{HKR}}(X; H, \omega(v)) = (-1)^{c(L) + \text{sign}(L)} Z_{\text{HKR}}(X; H, -\omega(v)).$$

Hence, up to a negative sign $Z_{\text{HKR}}(X; H, \omega(v))$ does not depend on the choice of a square root of $\mu_R(v)/\mu_R(v^{-1})$, in which case the invariant is more commonly written as:

$$Z_{\text{HKR}}(X; H) = [\mu_R(v)\mu_R(v^{-1})]^{-\frac{c(L)}{2}} [\mu_R(v)/\mu_R(v^{-1})]^{-\frac{\text{sign}(L)}{2}} \langle L \rangle_{H, \mu_R}.$$

Just as the Witten-Reshetikhin-Turaev invariant, Z_{HKR} can also be refined to an invariant of 3-manifolds endowed with a 2-framing. We recall the definition of a 2-framing introduced in [2]. Let N be a Riemannian manifold of dimension $n \geq 3$. Consider the diagonal embedding of $\text{SO}(n)$ into $\text{SO}(2n)$:

$$\begin{array}{ccccc} & & & & \text{Spin}(2n) \\ & & & \nearrow & \downarrow \pi \\ \text{SO}(n) & \xrightarrow{\quad} & \text{SO}(n) \times \text{SO}(n) & \longrightarrow & \text{SO}(2n) \end{array}$$

The embedding induces a lift from $\text{SO}(n)$ to $\text{Spin}(2n)$, indicated by the dashed arrow, so that the diagram above commutes. The diagram determines a spin structure of $2T_N := T_N \oplus T_N$, double of the tangent bundle of N . A 2-framing of N is defined to be a trivialization of $2T_N$ viewed as a $\text{Spin}(2n)$ bundle. For three manifolds, 2-framings are equivalent to p_1 structures [6]. Let X be a closed oriented 3-manifold. Since $\pi_1(\text{Spin}(6)) = \pi_2(\text{Spin}(6)) = 0$, $\pi_3(\text{Spin}(6)) = \mathbb{Z}$, the set of 2-framings of X form a torsor over $H^3(X; \pi_3(\text{Spin}(6))) \simeq \mathbb{Z}$. Choose any 4-manifold W whose boundary is X . For any 2-framing ϕ on X , define

$$\sigma(\phi) := 3\text{sign}(W) - \frac{1}{2}p_1(2T_W, \phi), \quad (40)$$

where $\text{sign}(W)$ is the Hirzebruch signature of W and $p_1(2T_W, \phi)$ is the relative Pontrjagin number.⁵ By the Hirzebruch signature formula for closed 4-manifolds, $\sigma(\phi)$ is independent of the bounding manifold W . Since $2T_X$ is spin, it implies $p_1(2T_W, \phi)$ is an even integer. Moreover, σ is an affine linear isomorphism from the set of the 2-framings to \mathbb{Z} . The canonical 2-framing is the unique ϕ_0 satisfying $\sigma(\phi_0) = 0$.

Let H, μ_R, v be as above, $\omega_6(v)$ be a sixth root of $\mu_R(v)/\mu_R(v^{-1})$ and $\omega(v) = \omega_6(v)^3$. The Z_{HKR} invariant for the pair (X, ϕ) is defined to be:

$$Z_{\text{HKR}}(X, \phi; H, \omega_6(v)) := (\mu_R(v)/\omega(v))^{-c(L)} \omega_6(v)^{-\frac{1}{2}p_1(2T_{W_L}, \phi)} \langle L \rangle_{H, \mu_R}, \quad (41)$$

where W_L is the 4-manifold obtained from the surgery link L . It follows immediately from the definitions that

$$Z_{\text{HKR}}(X, \phi; H, \omega_6(v)) = \omega_6(v)^{\sigma(\phi)} Z_{\text{HKR}}(X; H, \omega(v)). \quad (42)$$

Thus the original invariant is equal to the refined invariant evaluating at the canonical 2-framing. The chosen roots $\omega_6(v)$ and $\omega(v)$ are often dropped from the formula when they are clear from the context. In the following we use $Z_{\text{HKR}}(\cdot)$ to denote both the refined invariant and the original one.

⁵Note that the σ map defined here is equal to three times the σ invariant in [2].

4 Main Results I

In this section, H denotes a finite dimensional double balanced Hopf algebra. Hence its Drinfeld double $D(H) = H^{\text{cop}} \otimes H$ is ribbon. Note that $D(H)$ is also factorizable and unimodular. See Section 2 for our notations on Hopf algebras.

Theorem 4.1 (= Theorem 1.1). Let H be a finite dimensional double balanced Hopf algebra and X be a closed oriented 3-manifold, then there exist a framing b and a 2-framing ϕ of X such that,

$$Z_{\text{Kup}}(X, b; H) = Z_{\text{HKR}}(X, \phi; D(H)). \quad (43)$$

Proof. The proof is given in the next three subsections. Section 4.1 gives a special Heegaard diagram of X in which one family of circles form a surgery link for X . In Section 4.2, we construct a framing b of X presented on the Heegaard diagram and compute $Z_{\text{Kup}}(X, b; H)$. In Section 4.3 we define a 2-framing ϕ and compute $Z_{\text{HKR}}(X, \phi; D(H))$. The equality in the theorem then follows. \square

4.1 Special Heegaard Diagrams

A Heegaard diagram is a triple $R = (\Sigma_g, \alpha, \beta)$ where Σ_g is a closed oriented surface of genus g , and $\alpha = \{\alpha_1, \dots, \alpha_g\}$ (resp. $\beta = \{\beta_1, \dots, \beta_g\}$) is a collection of g disjoint simple closed curves such that the complement of the α_i 's (resp. the β_j 's) in Σ_g is a $2g$ -punctured sphere. A closed oriented 3-manifold is obtained from a Heegaard diagram by attaching 2-handles to the closed curves and filling sphere boundaries with 3-handles. Every closed oriented 3-manifold can be represented by a Heegaard diagram, and different diagrams of the same manifold are related by isotopy, handle slides and stabilization. A diagram $R = (\Sigma_g, \alpha, \beta)$ of the 3-sphere \mathbb{S}^3 is *standard* if the geometric intersection of α_i with β_j is 1 for $i = j$ and 0 otherwise. Every standard diagram of genus g for \mathbb{S}^3 is isotopic to the one obtained by taking stabilization g times from the two sphere. Heegaard diagrams with certain special properties are studied in [5].

Theorem 4.2. [5] Every closed oriented 3-manifold X has a Heegaard diagram $R = (\Sigma_g, \alpha, \beta)$ for some genus g satisfying the following properties:

1. There exists a collection of g curves $\gamma = \{\gamma_1, \dots, \gamma_g\}$ on Σ_g such that both $R_1 = (\Sigma_g, \alpha, \gamma)$ and $R_2 = (\Sigma_g, \beta, \gamma)$ are standard diagrams for \mathbb{S}^3 .
2. View β as a framed link in \mathbb{S}^3 determined by R_1 , where the framing is taken to be a parallel copy of β in the Heegaard surface. Then β is a surgery link for X . Moreover, the framings are all even integers.

Proof. (Sketch) See [5] for a more detailed proof. It is a standard result that X has a surgery link L which is the plat closure of a certain $2g$ -strand braid $\sigma \in B_{2g}$. Actually one can always choose σ to be a pure braid and the framing of each component to be an even integer. In this case, L has g components $\{L_1, \dots, L_g\}$. Assume σ is aligned vertically in the stripe $\{0\} \times \mathbb{R} \times [0, 1]$ with end points $(0, i, 0)$, $(0, i, 1)$, $i = 1, 2, \dots, 2g$. The i -th plat on the bottom

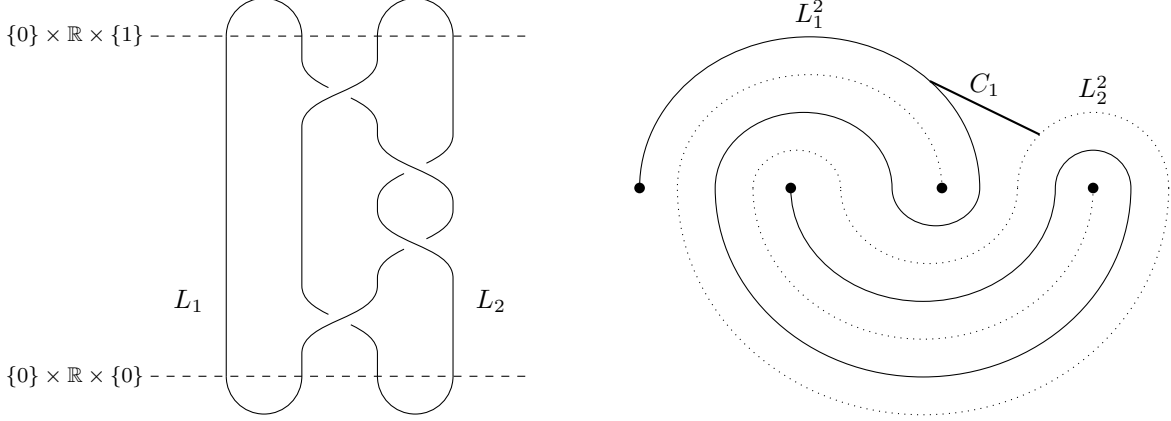


Figure 10: (Left) L is the plat closure of $\sigma = \sigma_2\sigma_3^{-2}\sigma_2$; (Right) The part of L in the plane $\mathbb{R}^2 \times \{1\}$ where L_i^1 (not drawn) is an arc lying inside the page connecting the $(2i - 1)$ -th dot and the $(2i)$ -th dot, $i = 1, 2$.

(resp. on the top) connects $(0, 2i - 1, 0)$ and $(0, 2i, 0)$ (resp. $(0, 2i - 1, 1)$ and $(0, 2i, 1)$). See Figure 10 (Left). According to Theorem 5.2 in [5], one can isotope L , by untwisting the braid at the cost of twisting the plats on the top, so that each L_i is decomposed as $L_i^1 \cup L_i^2$ (see Figure 10 (right)), where L_i^1 is the arc consisting of the segments $\{0\} \times \{2i - 1, 2i\} \times [0, 1]$ and the i -th plat on the bottom, and L_i^2 is an arc in $\mathbb{R}^2 \times \{1\}$ connecting $(0, 2i - 1, 1)$ and $(0, 2i, 1)$. Moreover, the L_i^2 's are disjoint from each other. Arbitrarily choose $g - 1$ mutually disjoint arcs C_1, \dots, C_{g-1} in the plane $\mathbb{R}^2 \times \{1\}$ so that C_j connects a point in L_j^2 to a point in L_{j+1}^2 and is otherwise disjoint from all the L_i^2 's. Let

$$B := \left(\bigcup_{i=1}^{g-1} C_i \right) \cup \left(\bigcup_{i=1}^g L_i^2 \right), \quad H := B \cup \left(\bigcup_{i=1}^g L_i^1 \right),$$

and $N(B)$ and $N(H)$ be a regular neighborhood of B and H , respectively. Then $N(B)$ is a 3-ball and $N(H)$ is a handlebody obtained from $N(B)$ by attaching g 1-handles, each of which corresponds to a regular neighborhood $N(L_i^1)$ of L_i^1 . Clearly $\mathbb{S}^3 = N(H) \cup N(H)^c$ is a Heegaard decomposition of \mathbb{S}^3 . On $\partial N(H)$ choose a complete set of meridian curves $\gamma = \{\gamma_1, \dots, \gamma_g\}$ for $N(H)$ and a complete set of meridian curves $\alpha = \{\alpha_1, \dots, \alpha_g\}$ for $N(H)^c$ so that $(\partial N(H), \alpha, \gamma)$ is a standard Heegaard diagram of \mathbb{S}^3 .

Let $\beta = \{\beta_1, \dots, \beta_g\}$ be a set of curves with β_i representing the framing of L_i . One can assume β_i is contained in $\partial N(H) \cap \partial N(L_i)$, where $N(L_i)$ is a regular neighborhood of L_i . It follows that the complement of β in $\partial N(H)$ is a $2g$ -punctured sphere. It can be shown that $(\partial N(H), \beta, \gamma)$ is a standard Heegaard diagram of \mathbb{S}^3 and that $(\partial N(H), \alpha, \beta)$ is a Heegaard diagram of X . Clearly L and β are isotopic framed links. \square

Theorem 4.2 provides a bridge between Heegaard diagrams and surgery links which is exactly the ingredient that will be used to compare Z_{Kup} and Z_{HKR} . For the sake of clarity, we give an explicit description of the Heegaard diagram/surgery link model.

Endow \mathbb{R}^3 with the $\{x, y, z\}$ coordinates. Let $\mathbb{S}^3 = \mathbb{R}^3 \cup \{\infty\}$, $B_+ = (\mathbb{R}^2 \times \mathbb{R}_{\geq 0}) \cup \{\infty\}$, $B_- = (\mathbb{R}^2 \times \mathbb{R}_{\leq 0}) \cup \{\infty\}$, and $\mathbb{S}^2 = B_+ \cap B_- = (\mathbb{R}^2 \times \{0\}) \cup \{\infty\}$. Also identify \mathbb{R}^2 with

$\mathbb{R}^2 \times \{0\} \subset \mathbb{S}^2$. Fix an integer $g \geq 0$. For $1 \leq i \leq g$, let D_i^1 and D_i^2 be the disks in \mathbb{S}^2 centered at $(0, i)$ and $(1, i)$, respectively, of radius $\epsilon \ll 1/8$, and let N_i be a three dimensional 1-handle in B_- connecting D_i^1 and D_i^2 . The N_i 's are unknotted and unlinked. For instance, one can push the segment $[0, 1] \times \{i\}$ slightly into B_- keeping the end points fixed and set N_i to be a regular neighborhood of the push-off. Set $B_{g,+} = B_+ \cup_{i=1}^g N_i$ and $B_{g,-} = B_- \setminus (\cup_{i=1}^g N_i)$, then $\mathbb{S}^3 = B_{g,+} \cup B_{g,-}$ is a standard genus- g Heegaard decomposition. Define $\Sigma_g := \partial B_{g,+} = \partial B_{g,-}$, $\partial N_i := \Sigma_g \cap N_i$, and $\mathbb{S}^{2;2g} := \Sigma_g \cap \mathbb{S}^2$. Clearly $\mathbb{S}^{2;2g}$ is a $2g$ -punctured sphere. We call ∂D_i^1 and ∂D_i^2 the left foot and right foot, respectively, of ∂N_i . The readers may find Figure 11 helpful in the following discussions. Take α_i to be a meridian of $B_{g,-}$ which consists of the segment $[\epsilon, 1 - \epsilon] \times \{i\}$ and the arc traveling through ∂N_i once (without twisting around N_i) connecting (ϵ, i) and $(1 - \epsilon, i)$. Also take γ_i to be a meridian of $B_{g,+}$ circling a section of N_i once. Let β_i be any simple closed curve in Σ_g which travels through ∂N_i once (without twisting around N_i) and spends the rest of time in $\mathbb{S}^{2;2g}$. Moreover, β_i is parallel to α_i when traveling in ∂N_i and all the β_i 's are disjoint from each other. Furthermore, each β_i crosses the segment $[\epsilon, 1 - \epsilon] \times \{i\}$ an even number of times. Define $\alpha = \{\alpha_1, \dots, \alpha_g\}$ and define β, γ analogously. Since β is contained in Σ_g , it can be naturally viewed as a framed link in \mathbb{S}^3 by taking a parallel copy in Σ_g as the framing curve. Furthermore, it has a diagram in \mathbb{S}^2 obtained by projecting the part of each β_i in ∂N_i to $[0, 1] \times \{i\}$ while keeping the part in $\mathbb{S}^{2;2g}$ fixed. See Figure 11 (Right). Denote the projection by $\tilde{\beta}$. With notations from above and by Theorem 4.2, we have

1. $(\Sigma_g, \alpha, \gamma)$ is a standard Heegaard diagram of \mathbb{S}^3 .
2. $\tilde{\beta}$ is a link diagram for β , and the self-linking number of each component of $\tilde{\beta}$ is an even integer.
3. $(\Sigma_g, \alpha, \beta)$ is a Heegaard diagram for the 3-manifold whose surgery link β . Denote such a 3-manifold by $X(\Sigma_g, \beta)$ with α and γ known implicitly. Then every closed oriented 3-manifold is homeomorphic to some $X(\Sigma_g, \beta)$.

4.2 A Framing on $X(\Sigma_g, \beta)$ and the Kuperberg Invariant

Given the 3-manifold $X = X(\Sigma_g, \beta)$, we construct a framing of X presented in the Heegaard diagram $(\Sigma_g, \alpha, \beta)$. Recall from Section 3.1 that a framing consists of two orthogonal combings b_1 and b_2 satisfying certain conditions, where b_1 is represented as a vector field with $2g + 1$ singularities and b_2 is represented as a set of twist fronts. For $1 \leq i \leq g$, let w_i be the winding number of $\tilde{\beta}_i$. Since the framing of $\tilde{\beta}_i$ is even, then w_i is odd. Set $w_i = 2n_i + 1$.

First combing b_1 : the construction of b_1 is generalized from that given in [8]. We describe the flow lines and singularities of b_1 . The singularities are located at $a_i^l := (1/4, i)$, $a_i^u = (3/4, i)$, and ∞ , $i = 1, \dots, g$. All the singularities have index -1 except the one at ∞ which has index 2. Let R_i be the open rectangle $(-1, 2) \times (i - 1/2, i + 1/2)$ and $R = \sqcup_{i=1}^g R_i$. In $\mathbb{R}^2 \setminus R$, b_1 takes the value $\frac{\partial}{\partial x}$, i.e., b_1 points toward the positive direction of the x -axis⁶. Note that on the boundary of each R_i , the value of b_1 is $\frac{\partial}{\partial x}$. Now it suffices to describe b_1 inside R_i

⁶It is direct to check this implies ∞ is a singular point of index 2.

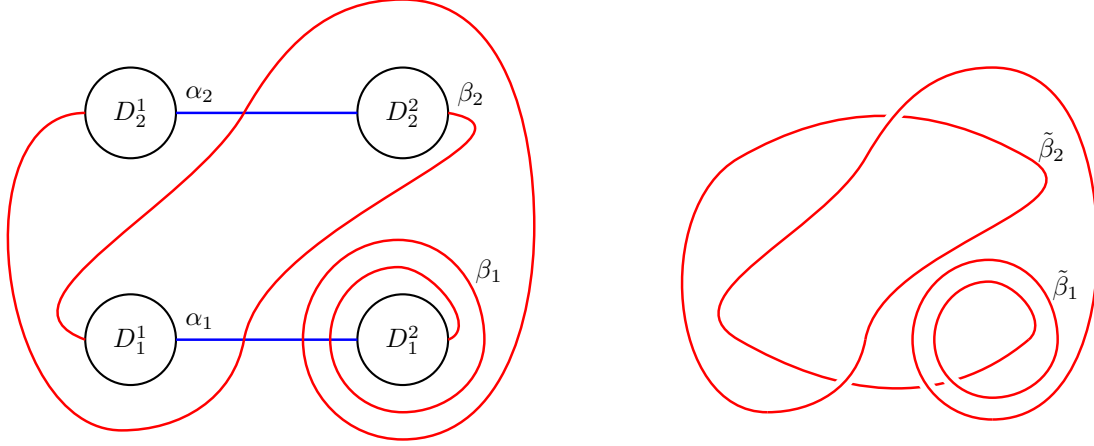


Figure 11: (Left) The x - y plane. α and β are represented by arcs in blue and red, respectively. The 1-handles N_i 's are outside of the plane. (Right) The diagram $\tilde{\beta}$ in x - y plane of β viewed as a link.

and ∂N_i . This is illustrated in Figure 12, where dashed lines represent the flow lines and C_i is the circle centered at $(0, i)$ with radius 2ϵ . The behavior of b_1 inside the annulus bounded by C_i and ∂D_i^1 is as follows. The field b_1 points toward the center on C_i and ∂D_i^1 . Along each radial segment connecting C_i and ∂D_i^1 , b_1 rotates counterclockwise, in unit $1 = 360^\circ$, by the degree n_i .⁷ If we set the center of C_i to be $(0, 0)$ for simplicity, then a formula of b_1 inside the annulus is given by:

$$b_1(x, y) = -\cos\left(\theta + 2\pi n_i \frac{2\epsilon - r}{\epsilon}\right) \frac{\partial}{\partial x} - \sin\left(\theta + 2\pi n_i \frac{2\epsilon - r}{\epsilon}\right) \frac{\partial}{\partial y}, \quad (44)$$

where (r, θ) is the polar coordinate of (x, y) . Note that the radial segments are not flow lines. Figure 13 shows a model of flow lines for $n_i = 1$. The rotation of any degree can be obtained by stacking this model or the orientation reversal model in the radial direction. Inside the tube ∂N_i the flow lines of b_1 travel from one end to the other without any twisting and emerges out of ∂D_i^2 .

Second combing \mathbf{b}_2 : for $1 \leq i \leq g$, there are $|w_i|$ twist fronts, each of which travels through ∂N_i in parallel and connects the two singularities a_i^l and a_i^u . See Figure 14. The (small triangles on) twist fronts point upward as shown in the figure if $w_i > 0$ and downward otherwise.

Lower and upper circles: we designate α and β as the set of lower and upper circles, respectively. But note that we need each circle to pass exactly one singular point of index -1 in a specific manner (see Section 3.1). We achieve this by perform a slight perturbation on the circles. See Figure 15. For each i , set the base point of α_i to be a_i^l and orient α_i so that it points to the positive x -direction (horizontally to the right in the figure) at a_i^l . Then perturb α_i off a_i^u and perturb β_i so that it passes a_i^u . Set a_i^u as the base point of β_i . The orientation is chosen so that it points upward at a_i^u .

⁷If $n_i < 0$, then the rotation is clockwise of degree $-n_i$.

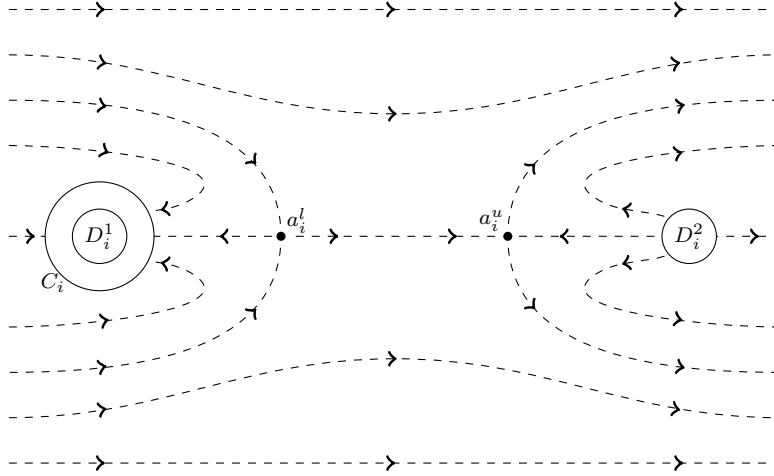


Figure 12: Flow lines of b_1 in the closed rectangle $\overline{R}_i = [-1, 2] \times [i - 1/2, i + 1/2] \subset \mathbb{R}^2$.

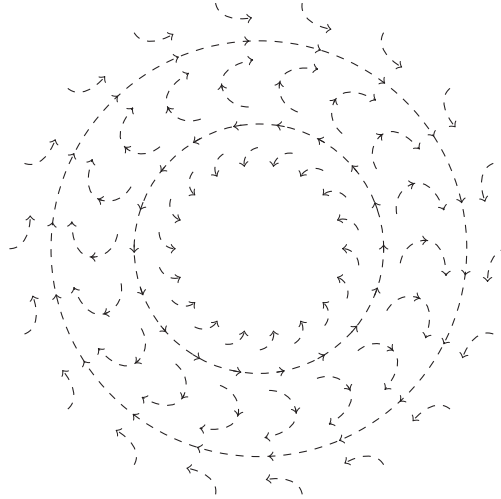


Figure 13: A model of b_1 rotation in the annulus between C_i and ∂D_i^1 for $n_i = 1$. The two circles are closed flow lines, but not C_i and ∂D_i^1 .

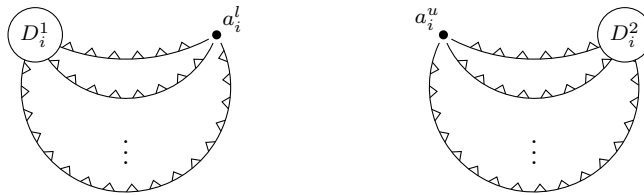


Figure 14: Twist fronts of b_2 connecting a_i^l and a_i^u in the case $w_i > 0$.

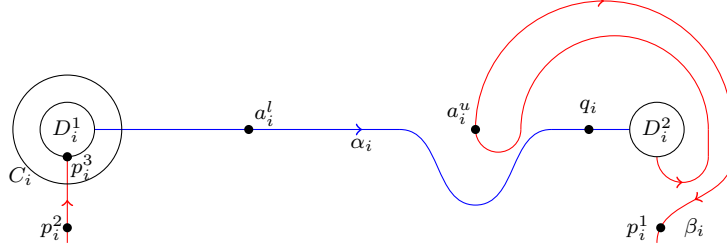


Figure 15: Perturbations, base points, and orientations of lower and upper circles

By isotopy, we may assume that each β_i is away from the feet of all ∂N_j 's and from all base points except the part as shown in Figure 15. In particular, all the intersections of the lower circles with upper circles are constrained in the horizontal segments connecting a lower base point to the corresponding upper base point. At the intersections, the upper circles are vertical. Recall from Section 3.1 the definitions of θ_c , $\theta_c(p)$, ϕ_c , $\phi_c(p)$. Let p, q be two points on a lower or upper circle c and define $\theta_c(p, q) = \theta_c(q) - \theta_c(p)$, namely, $\theta_c(p, q)$ is the degree of rotation of c' relative to b_1 from p to q along c .

Lemma 4.3. • Let p_i^1, p_i^2, p_i^3 be points on β_i as shown in Figure 15, then

$$\theta_{\beta_i}(a_i^u, p_i^1) = \theta_{\beta_i}(p_i^1) = -\frac{1}{4}, \quad \theta_{\beta_i}(p_i^2, p_i^3) = -\frac{1}{4} - n_i, \quad \theta_{\beta_i}(p_i^3, a_i^u) = -\frac{1}{2}. \quad (45)$$

- Let q_i be a point on α_i as shown Figure 15, then $\theta_{\alpha_i}(q_i) = \frac{1}{2}$.
- Let p be a point on β_i between p_i^1 and p_i^2 and assume the tangent of β_i at p is vertical, then $\theta_{\beta_i}(p_i^1, p) = \frac{w_p}{2}$, where w_p (also see Section 3.2) is the algebraic sum of extrema along β_i between p_i^1 to p , where an extremum is counted as $+1$ if the orientation near it is counterclockwise, and as -1 otherwise.

Proof. The first two parts follow directly from observations of Figure 12 and 15. In particular, $\theta_{\beta_i}(p_i^2, p_i^3)$ would be $-\frac{1}{4}$ if the flow lines inside the annulus between C_i and ∂D_i^1 did not rotate. The rotations in the annulus by the degree n_i contributes an extra $-n_i$ to $\theta_{\beta_i}(p_i^2, p_i^3)$. The third part is obtained by noting that when traveling along β_i away from all base points, each pass of an extremum contributes $\pm\frac{1}{2}$ to $\theta_{\beta_i}(p_i^1, p)$ depending on the orientation near the extremum. Also see Lemma 1 in [7]. \square

Lemma 4.4. For the combings b_1, b_2 constructed above, we have

$$\theta_{\alpha_i} = \phi_{\alpha_i} = n_i + \frac{1}{2}, \quad \theta_{\beta_i} = -\phi_{\beta_i} = n_i + \frac{1}{2}, \quad 1 \leq i \leq g. \quad (46)$$

Proof. By the third part of Lemma 4.3, we have $\theta_{\beta_i}(p_i^1, p_i^2) = w_i + \frac{1}{2}$, where w_i is the winding number of $\tilde{b}\alpha_i$. Hence,

$$\begin{aligned} \theta_{\beta_i} &= \theta_{\beta_i}(a_i^u, p_i^1) + \theta_{\beta_i}(p_i^1, p_i^2) + \theta_{\beta_i}(p_i^2, p_i^3) + \theta_{\beta_i}(p_i^3, a_i^u) \\ &= \left(-\frac{1}{4}\right) + \left(w_i + \frac{1}{2}\right) + \left(-\frac{1}{4} - n_i\right) + \left(-\frac{1}{2}\right) = n_i + \frac{1}{2}. \end{aligned}$$

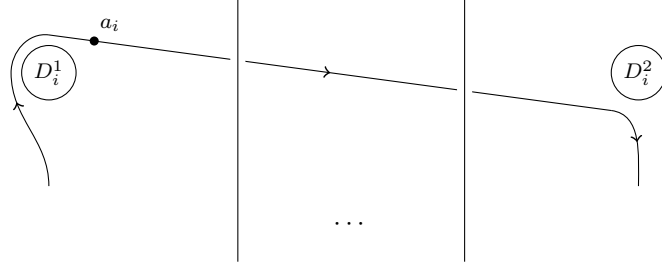


Figure 16: A perturbation of the diagram $\tilde{\beta}$.

For θ_{α_i} , note that when traveling along α_i from q_i to a_i^l , we will cross the annulus between ∂D_i^1 and C_i , and the direction of the crossing is from ∂D_i^1 to C_i . During this crossing, the vector field b_1 rotates by a degree of $-n_i$, and hence θ_{α_i} increases by n_i . Then the equality $\theta_{\alpha_i} = n_i + \frac{1}{2}$ follows from the second part of Lemma 4.3.

The equalities concerning the ϕ 's are derived by counting the number of crossings of the circles with twist fronts. \square

By Lemma 4.4, the combings b_1, b_2 extend to a framing on X . Denote this framing by $b = (b_1, b_2)$.

Lemma 4.5. Let p be a crossing of β_i with α_j , then $\theta_{\alpha_j}(p) = \phi_{\alpha_j}(p) = \phi_{\beta_i}(p) = 0$, and $\theta_{\beta_i}(p) = -\frac{1}{4} + \frac{w_p}{2}$, where w_p is defined as in the third part of Lemma 4.3. In particular, in the tensor network computing $Z_{\text{Kup}}(X, b; H)$, the tensor assigned to p is $S^{\theta(p)}T^{\phi(p)}$ where $\theta(p) = 1 - w_p$ and $\phi(p) = 0$.

The Kuperberg invariant $Z_{\text{Kup}}(X, b; H)$ can be described as follows. Assign the tensors in Figure 8 to each α_i , each β_j , and each crossing p , with $\phi_i = n_i + \frac{1}{2}$, $\phi^j = -n_j - \frac{1}{2}$, $\phi(p) = 0$, and $\theta(p) = 1 - w_p$.

4.3 Computing Z_{HKR}

We compute Z_{HKR} for the 3-manifold $X = X(\Sigma_g, \beta)$ from $D(H)$. See Section 2 and 3.2 for some notations to be used below. Recall from Section 4.1 that a surgery link diagram for X is $\tilde{\beta}$. We perturb $\tilde{\beta}$ slightly so that the y -coordinate function serves as a height function for $\tilde{\beta}$. The perturbed diagram, still denoted by $\tilde{\beta}$, is shown in Figure 16. That is, instead of connecting the two feet $\partial D_i^1, \partial D_i^2$ horizontally, $\tilde{\beta}_i$ travels from slightly over the top of D_i^1 to slightly below the bottom of D_i^2 in a right-downwards direction. We also assume all the crossings are right-handed and are constrained in the segments $\sqcup_{i=1}^g (1/4, 3/4) \times \{i\}$. Pick a point a_i on $\tilde{\beta}_i$ near the left feet ∂D_i^1 (past the maximum) as the base point of $\tilde{\beta}_i$ and orient $\tilde{\beta}_i$ so that it points to the right feet ∂D_i^2 at a_i . Under this orientation, we have $\delta_i = 0$.

We use tensor network formulation to compute $\langle \tilde{\beta} \rangle_{D(H), \mu_R^D}$. Recall that in $D(H)$, each leg in a tensor consists of two lines, one corresponding to $H^{*\text{cop}}$ and the other to H . The $(R^D)^{-1}$ tensor is assigned to all crossings since they are all right-handed. See Figure 17. A dot at the end of a leg indicates a position where tensors will be contracted later. Note that here two neighboring dots are treated as one dot since we are working with tensors in $D(H)$. Call a dot *covariant* if the leg attached to it is incoming and *contravariant* otherwise. We examine

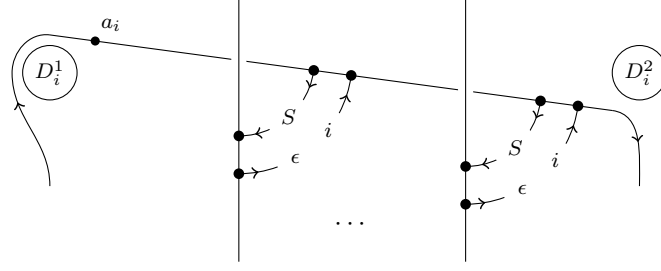


Figure 17: An assignment of R tensor to each crossing

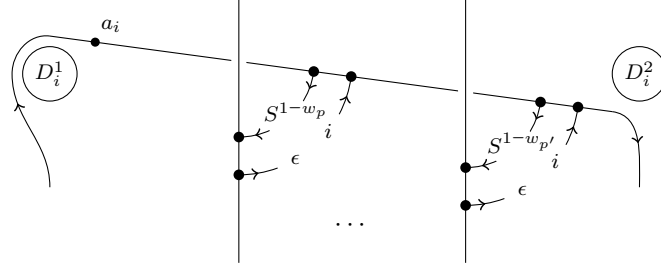


Figure 18: Combining the R tensor and S -tensor.

the S -tensor assigned to each dot. Each dot on a horizontal segment has an S^D power of 0 since there are no extrema between the base point to where the dot is located. For a dot on a vertical segment corresponding to a crossing p , assume it belongs to some $\tilde{\beta}_i$, then its S^D power is $-w_p$ where w_p is the algebraic sum of extrema between a_i and the dot. Note that $S_D^{-w_p}(\epsilon \otimes x) = \epsilon \otimes S^{-w_p}(x)$. Combining the R -tensor and S -tensor, the configuration now is as in Figure 18. Finally we apply the \tilde{M} tensor in Figure 9 to each $\tilde{\beta}_i$. This is broken down to several stages. Start from the base point a_i and travel along $\tilde{\beta}_i$ following its direction. One first comes across dots on the horizontal segment, and then dots on vertical segments. Firstly, multiplying the elements on the horizontal segments is equivalent to attaching a Δ -type tensor in Equation 10 (Left) with each outgoing leg corresponding to a contravariant dot from left to right. Secondly, multiplying elements on the vertical segments is equivalent to attaching an M -type tensor in Equation 10 (Right) with each incoming leg corresponding to a covariant dot, which again corresponds to the crossings on $\tilde{\beta}_i$. See Figure 19. Recall that $w_i = 2n_i + 1$ is the winding number of $\tilde{\beta}_i$. Finally, the whole \tilde{M} -tensor is obtained by multiplying the two dots on the top (Figure 19), the two dots on the bottom (Figure 19), and the element $(a^D)^{-n_i} = \alpha^{n_i} \otimes a^{-n_i}$, followed by the application of $\mu_R^D = e_L \otimes \mu_R$. Note that for $f \in H^*, x \in H$,

$$\mu_R^D((f \otimes i)(\epsilon \otimes x)(\alpha^{n_i} \otimes a^{-n_i})) = \mu_R^D((f \otimes x)(\alpha^{n_i} \otimes a^{-n_i})) = f(e_{n_i + \frac{1}{2}})\mu_{-n_i - \frac{1}{2}}(x)q^{n_i}$$

where the second equality is by Lemma 2.2. Therefore, the link evaluation $\langle \tilde{\beta} \rangle_{D(H), \mu_R^D}$ equals $q^{\sum_{i=1}^g n_i}$ times the tensor contraction as shown in Figure 20 with the latter one being exactly $Z_{\text{Kup}}(X, b; H)$ described in Section 4.2.

Finally, note that $\mu_R^D(v^D) = \tau^{-5}$ and $\mu_R^D((v^D)^{-1}) = \tau$. Choose τ^{-3} as the square root of $\mu_R^D(v^D)/\mu_R^D((v^D)^{-1})$. Hence, the Hennings-Kauffman-Radford invariant (the non-refined

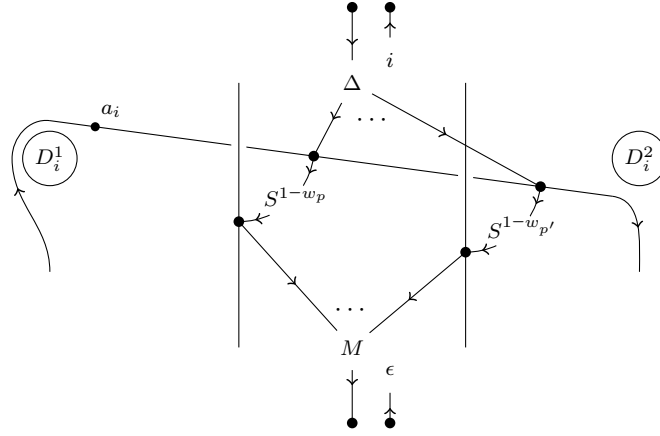


Figure 19: Assignment of \widetilde{M} tensor

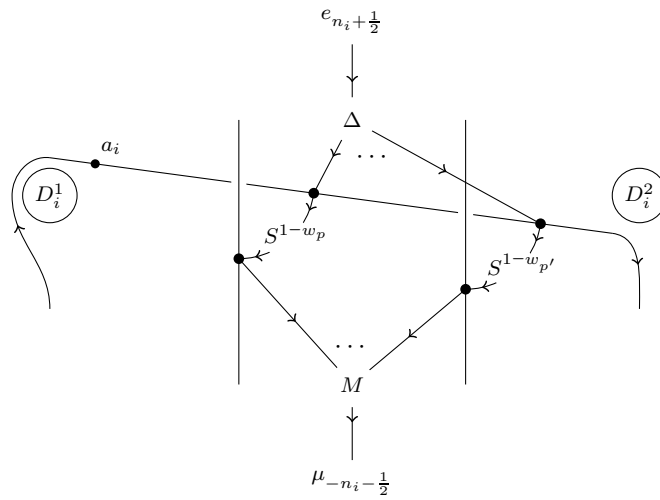


Figure 20: Contraction of the R , S , and \widetilde{M} tensors

version) is given by:

$$Z_{\text{HKR}}(X; D(H), \tau^{-3}) = \tau^{3\text{sign}(\tilde{\beta})+2\sum_{i=1}^g w_i} Z_{\text{Kup}}(X, b; H). \quad (47)$$

Now choose τ^{-1} as the sixth root of $\mu_R^D(v^D)/\mu_R^D((v^D)^{-1})$. Let ϕ be the 2-framing of X such that $\sigma(\phi) = 3\text{sign}(\tilde{\beta}) + 2\sum_{i=1}^g w_i$. Then we get

$$Z_{\text{HKR}}(X, \phi; D(H), \tau^{-1}) = Z_{\text{Kup}}(X, b; H). \quad (48)$$

5 Main Results II

In this section, the Hopf algebra H is assumed to be factorizable and ribbon. It follows that H is unimodular. We turn to another relation between Z_{Kup} and Z_{HKR} . It can be viewed as the dual of the relation in Theorem 4.1. That is, instead of taking the double of H , we take the double $D(X) = X \# \overline{X}$ of the 3-manifold X in Z_{HKR} , where \overline{X} is the manifold X with opposite orientation.

Theorem 5.1 (= Theorem 1.2). Let H be a finite dimensional factorizable ribbon Hopf algebra and X be a closed oriented 3-manifold, then there exists a framing b of X such that

$$Z_{\text{Kup}}(X, b; H) = Z_{\text{HKR}}(X \# \overline{X}; H). \quad (49)$$

The main tool in topology to establish Theorem 5.1 is the chain-mail link. A surgery diagram of $X \# \overline{X}$ is obtained from a Heegaard diagram of X by pushing the upper circles into the lower handle body slightly. Then the upper circles and the lower circles form a link $L_{D(X)}$, called a chain-mail link [35]. All these curves are framed by thickening them into thin bands parallel to the Heegaard surface. The framed link $L_{D(X)}$ is a surgery link for $D(X)$. For instance, Figure 21 shows the diagram of the chain-mail link for the Heegaard diagram in Figure 11.

Note that the signature $\sigma(L_{D(X)})$ of the chain-mail link is always zero [35] and it is possible to choose μ_R such that $\mu_R(v)\mu_R(v^{-1}) = 1$ in a factorizable ribbon Hopf algebra [12]. Hence with such a choice of μ_R and a suitable choice $\omega(v)$ of a square root of $\mu_R(v)/\mu_R(v^{-1})$, the normalization factor in defining Z_{HKR} is

$$[\mu_R(v)\mu_R(v^{-1})]^{-\frac{c(L_{D(X)})}{2}} [\mu_R(v)/\mu_R(v^{-1})]^{-\frac{\sigma(L_{D(X)})}{2}} = 1.$$

Thus $Z_{\text{HKR}}(X \# \overline{X}; H) = \langle L_{D(X)} \rangle_{H, \mu_R}$.

Take X to be $X(\Sigma_g, \beta)$ and choose the framing b to be the one defined in Section 4.2. We prove $Z_{\text{Kup}}(X, b; H) = \langle L_{D(X)} \rangle_{H, \mu_R}$. Similar to the proof of Theorem 4.1 in Section 4.3, we perturb the diagram of $L_{D(X)}$, and choose orientation and base point for each component as shown in Figure 22. The following lemma is proved in [8]. Note that we have an extra S factor (RHS of Figure 23) compared to the statement in [8]. This is due to the use of a slightly different but equivalent convention in current paper. It is also not hard to verify the lemma directly.

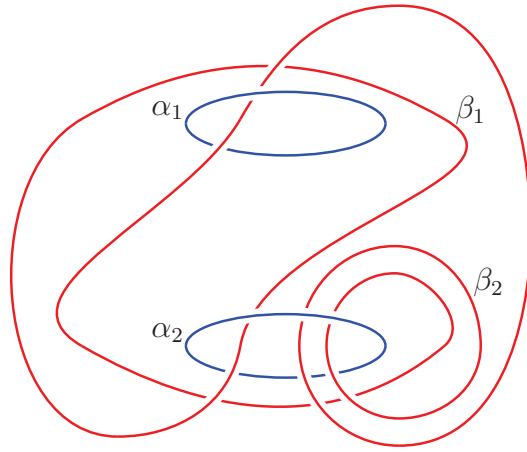


Figure 21: The chain-mail link corresponding to the Heegaard diagram in Figure 11

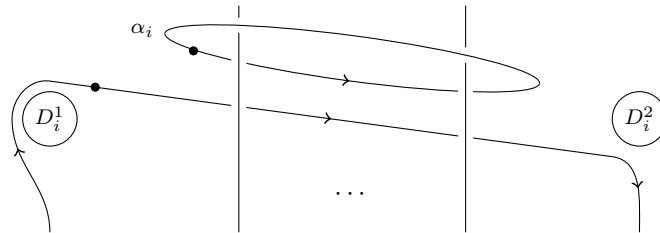


Figure 22: Diagram of a chain-main link.

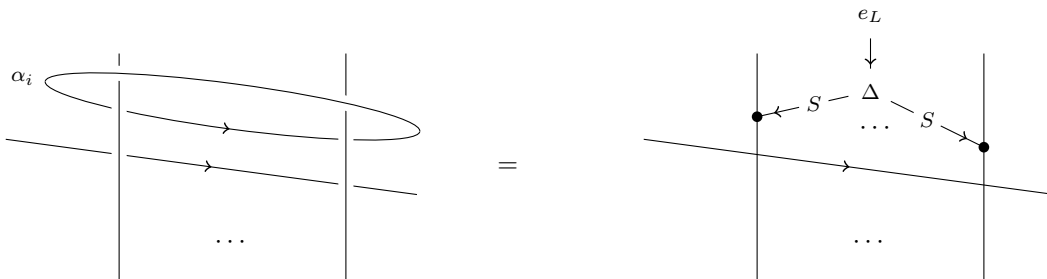


Figure 23: Tensor replacement in computing Z_{HKR} . Please be warned that the outgoing legs of the Δ tensor here is enumerated counterclockwise, in contrast to the default clockwise ordering.

Lemma 5.2. The equality in Figure 23 holds, where the equality means when the diagram on the LHS is assigned tensors according to the rules defining Z_{HKR} , then contracting the tensors results in the one on the RHS.

Since H is unimodular, we have $e_{n-1/2} = e_L$ for any integer n . Lemma 5.2 shows that the linking between the lower and upper circles results in the Δ tensor (Figure 8) with an additional S action on each outgoing leg. This effect is the same as assigning the Δ tensor to the lower circle (with an additional S -action). Now for the dot (Figure 23) corresponding to a crossing p , the S powers assigned to it is S^{-w_p} . Combining the extra S factor from the previous step, we get S^{1-w_p} , which is the correct tensor assigned to the crossing p in the Kuperbeg invariant (see the end of Section 4.2). Finally, the M -tensor in the Z_{HKR} is equal to the M -tensor in the Z_{Kup} :

$$\begin{array}{c}
 \begin{array}{ccc}
 & \searrow & \\
 \vdots & & \\
 & \nearrow & \\
 G^{1-w_i} & \longrightarrow & M \longrightarrow \mu_R
 \end{array}
 & = &
 \begin{array}{ccc}
 & \searrow & \\
 \vdots & & \\
 & \nearrow & \\
 & \longrightarrow & M \longrightarrow \mu_{-n_i-1/2}
 \end{array}
 \end{array}$$

We get $\langle L_{D(X)} \rangle_{H, \mu_R} = Z_{\text{Kup}}(X, b; H)$.

Acknowledgment The authors would like to thank Greg Kuperberg, Siu-Hung Ng, and Zhengnan Wang for helpful discussions. LC is supported by NSFC Grant No. 11701293. SXC acknowledges the support from the Simons Foundation.

References

- [1] Michael Atiyah. Topological quantum field theories. *Publications Mathématiques de l'IHÉS*, 68(1):175–186, 1988.
- [2] Michael Atiyah. On framings of 3-manifolds. *Topology*, 29(1):1–7, 1990.
- [3] John Barrett and Bruce Westbury. The equality of 3-manifold invariants. In *Mathematical Proceedings of the Cambridge Philosophical Society*, volume 118, pages 503–510. Cambridge University Press, 1995.
- [4] John Barrett and Bruce Westbury. Invariants of piecewise-linear 3-manifolds. *Transactions of the American Mathematical Society*, 348(10):3997–4022, 1996.
- [5] Joan Birman and Jerome Powell. Special representations for 3-manifolds. In *Geometric topology (Proc. of 1977 Georgia Topology Conf.)*, pages 23–51, 1977.
- [6] Christian Blanchet, Nathan Habegger, Gregor Masbaum, and Pierre Vogel. Topological quantum field theories derived from the Kauffman bracket. *Topology*, 34(4):883–927, 1995.
- [7] Liang Chang. A new proof of $Z_{\text{Kup}} = |Z_{\text{Hem}}|^2$ for semisimple hopf algebras. *arXiv:1504.00743*, 2015.

- [8] Liang Chang and Zhenghan Wang. $|Z_{Kup}| = |Z_{Henn}|^2$ for lens spaces. *Quantum Topology*, (4):1–35, 2013.
- [9] Qi Chen and Thomas Kerler. Integrality and gauge dependence of Hennings TQFTs. *Journal of Pure and Applied Algebra*, 2017.
- [10] Qi Chen, Srikanth Kuppum, and Parthasarathy Srinivasan. On the relation between the WRT invariant and the Hennings invariant. In *Mathematical Proceedings of the Cambridge Philosophical Society*, volume 146, pages 151–163. Cambridge University Press, 2009.
- [11] Qi Chen, Chih-Chien Yu, and Yu Zhang. Three-manifold invariants associated with restricted quantum groups. *Mathematische Zeitschrift*, 272(3):987–999, 2012.
- [12] Miriam Cohen and Sara Westreich. Fourier transforms for Hopf algebras. *Contemp. Math.*, 433:115–133, 2007.
- [13] Shawn X Cui, Michael H Freedman, Or Sattath, Richard Stong, and Greg Minton. Quantum max-flow/min-cut. *Journal of Mathematical Physics*, 57(6):062206, 2016.
- [14] Marco De Renzi, Nathan Geer, and Bertrand Patureau-Mirand. Renormalized Hennings invariants and 2 + 1-TQFTs. *arXiv preprint arXiv:1707.08044*, 2017.
- [15] Alexander Doser, McKinley Gray, Winston Cheong, and Stephen F Sawin. Relationship of the Hennings and Chern-Simons invariants for higher rank quantum groups. *arXiv:1701.01423*, 2017.
- [16] Vladimir Drinfeld. Quantum groups. In *Proc. Int. Congr. Math.*, volume 1, pages 798–820, 1986.
- [17] Mark Hennings. Invariants of links and 3-manifolds obtained from Hopf algebras. *Journal of the London Mathematical Society*, 54(3):594–624, 1996.
- [18] Vaughan FR Jones. A polynomial invariant for knots via von Neumann algebras. *Bulletin of the American Mathematical Society*, 12(1):103–111, 1985.
- [19] Yevgenia Kashina, Susan Montgomery, and Siu-Hung Ng. On the trace of the antipode and higher indicators. *Israel Journal of Mathematics*, 188(1):57–89, 2012.
- [20] Yevgenia Kashina, Yorck Sommerhaeuser, and Yongchang Zhu. *On higher Frobenius-Schur indicators*, volume 181. American Mathematical Soc., 2006.
- [21] Louis H Kauffman and David E Radford. A necessary and sufficient condition for a finite-dimensional Drinfeld double to be a ribbon Hopf algebra. *Journal of Algebra*, 159(1):98–114, 1993.
- [22] Louis H Kauffman and David E Radford. Invariants of 3-manifolds derived from finite dimensional Hopf algebras. *J. Knot Theory Ramifications*, 4(1):131–162, 1995.

- [23] Thomas Kerler. Genealogy of nonperturbative quantum-invariants of 3-manifolds: The surgical family. *arXiv q-alg/9601021*, 1996.
- [24] Thomas Kerler. On the connectivity of cobordisms and half-projective TQFT's. *Communications in mathematical physics*, 198(3):535–590, 1998.
- [25] Thomas Kerler. Homology TQFTs and the Alexander-Reidemeister Invariant of 3-Manifolds via Hopf Algebras and Skein Theory. *Canad. J. Math*, 55(4):766–821, 2003.
- [26] Greg Kuperberg. Involutory Hopf algebras and 3-manifold invariants. *International Journal of Mathematics*, 2(01):41–66, 1991.
- [27] Greg Kuperberg. Non-involutive Hopf algebras and 3-manifold invariants. *Duke Math. J.*, 84(1):83–129, 1996.
- [28] Volodymyr Lyubashenko. Modular transformations for tensor categories. *Journal of Pure and Applied Algebra*, 98(3):279–327, 1995.
- [29] Volodymyr V Lyubashenko. Invariants of 3-manifolds and projective representations of mapping class groups via quantum groups at roots of unity. *Communications in mathematical physics*, 172(3):467–516, 1995.
- [30] Jun Murakami. Generalized Kashaev invariants for knots in three manifolds. *Quantum Topology*, 8(1):35–73, 2017.
- [31] Román Orús. A practical introduction to tensor networks: Matrix product states and projected entangled pair states. *Annals of Physics*, 349:117–158, 2014.
- [32] David E Radford. The trace function and Hopf algebras. *Journal of Algebra*, 163(3):583–622, 1994.
- [33] David E Radford. *Hopf algebras*, volume 49. World Scientific, 2012.
- [34] Nicolai Reshetikhin and Vladimir G Turaev. Invariants of 3-manifolds via link polynomials and quantum groups. *Inventiones mathematicae*, 103(1):547–597, 1991.
- [35] Justin Roberts. Skein theory and Turaev-Viro invariants. *Topology*, 34(4):771–787, 1995.
- [36] Stephen F Sawin. Invariants of spin three-manifolds from Chern-Simons theory and finite-dimensional Hopf algebras. *Advances in Mathematics*, 165(1):35–70, 2002.
- [37] Matthew Sequin. *Comparing invariants of 3-manifolds derived from Hopf algebras*. The Ohio State University, 2012.
- [38] Maksim Valer'evich Sokolov. Which lens spaces are distinguished by Turaev-Viro invariants. *Mathematical Notes*, 61(3):384–387, 1997.
- [39] Vladimir Turaev. Quantum invariants of 3-manifold and a glimpse of shadow topology. *Quantum groups*, pages 363–366, 1992.

- [40] Vladimir Turaev and Alexis Virelizier. On two approaches to 3-dimensional TQFTs. *arXiv:1006.3501*, 2010.
- [41] Vladimir G Turaev and Oleg Ya Viro. State sum invariants of 3-manifolds and quantum 6j-symbols. *Topology*, 31(4):865–902, 1992.
- [42] Kevin Walker. On Wittens 3-manifold invariants. 1991.
- [43] Edward Witten. Topological quantum field theory. *Communications in Mathematical Physics*, 117(3):353–386, 1988.